35th Annual International Conference of the IEEE EMBS
Osaka, Japan, 3 - 7 July, 2013

A Multi-Electrode Array Coupled with Fiberoptic for Deep-Brain Optical Neuromodulation and Electrical Recording

Songchao Guo, Hong Zhou, Jiacheng Zhang, Kedi Xu* and Xiaoxiang Zheng

Abstract— **In this paper we developed an integrated device comprised of a multi-electrode array coupled with optical fiber for deep-brain optical stimulation and electrical recording. We characterized the array device both electrically and optically, and conducted *in vivo* experiments on free moving rats for validation. This design of array device provides a viable tool for neuromodulation and neural signal acquisition in optogenetics and in other fields of neuroscience studies perspectively.**

I. Introduction

Optogenetics is a powerful tool for neural interfaces both upon brain functional studies and brain-machine interactions[1-3]. The light-sensitive channel protein, for example, Channelrhodopsin-2 (ChR2)[1], can be genetically expressed on specific type of neural population via specifically designed virus. These opsin transduced neurons can be further activated via optical stimulations at certain wavelengths[4]. Compared with traditional deep brain electrical stimulation[5-7], optogenetics provides an opportunity to record the neural electrical activity during the optical stimulus. Both optical stimulation and electrical recording for *in vivo* studies require robust devices. Recently several innovative devices upon microelectrode arrays (MEAs) combined with tip-modified optrodes have been reported[8-10], which, however, focus mainly upon studies on cortex areas. In this paper we reported an integrated array device for optical stimulation combined with electrical recording in deep-brain areas, which is less-invasive, brain-area independent, optical-fiber flexible, and, sensitive to different depths in brain, providing more dimensional information for light-induced neural activities.

The work of this article was supported by grants from the National Basic Research Program of China (2011CB504400), the National Natural Science Foundation (NSF) of China (61031002) , the National High Technology Research and Development Program of China (2012AA011602), the National NSF of China (61233015, 61001172, 61003150), the Specialized Research Fund for the Doctoral Program of Higher Education (20100101120104), and the Fundamental Research Funds for the Central Universities.

Songchao Guo is with Qiushi Academy for Advanced Studies (QAAS), Zhejiang University, Hangzhou 310027, China.

Hong Zhou is with Qiushi Academy for Advanced Studies (QAAS), Zhejiang University, Hangzhou 310027, China.

Jiacheng Zhang is with Qiushi Academy for Advanced Studies (QAAS), Zhejiang University, Hangzhou 310027, China.

*Kedi Xu is with Qiushi Academy for Advanced Studies (QAAS), Zhejiang University, Hangzhou 310027, China. (email:xukd@zju.edu.cn; phone/fax: +86 571 87952865)

Xiaoxiang Zheng is with Qiushi Academy for Advanced Studies (QAAS), Zhejiang University, Hangzhou 310027, China.

II. Materials and Methods

A. The Model of Light Transmission in the Brain Tissue

To design the array device, it is crucial to arrange the electrodes into substantial brain area where light-induced neural electric activities can be recorded, that is, the electrodes ought to be arranged with appropriate depth from the light source in the brain. Light transmission fraction was then required, which was calculated as the power with brain tissue present divided by the power without brain tissue present. We modeled using the Kubelka-Munk model for diffuse scattering media[9] as Equation (1) and assumed that no absorption occurs in the process:

$$T = \frac{1}{Sz+1} \tag{1}$$

where T is the transmission fraction, z is the light penetration distance from the light source in brain, and S is the scatter coefficient per unit distance of light penetration, which is 11.2mm^{-1} for mouse and 10.3mm^{-1} for rat[9]. Moreover, to estimate the complete relationship between light intensity and the penetration distance z in brain tissue, it is necessary to take into consideration the fractional decrease due to the conical geometry of light at distance z in the absence of tissue scattering and absorption[9]. The geometric decrease in light intensity with relation to the penetration distance z can be calculated as:

$$\frac{I(z)}{I(z=0)} = \frac{\rho^2}{(z+\rho)^2} \tag{2}$$

in which

$$\rho = r\sqrt{(\frac{n_{tis}}{NA_{fib}})^2 - 1} \tag{3}$$

where r denotes the radius of the fiber, NA_{fib} the numerical aperture of the fiber, and n_{tis} the refraction index of the gray matter tissue with the value of 1.36. Altogether we derived the model for estimating light transmission loss in the brain tissue, mainly caused by the scattering and geometrical losses:

$$\frac{I(z)}{I(z=0)} = \frac{\rho^2}{(Sz+1)(z+\rho)^2}. \tag{4}$$

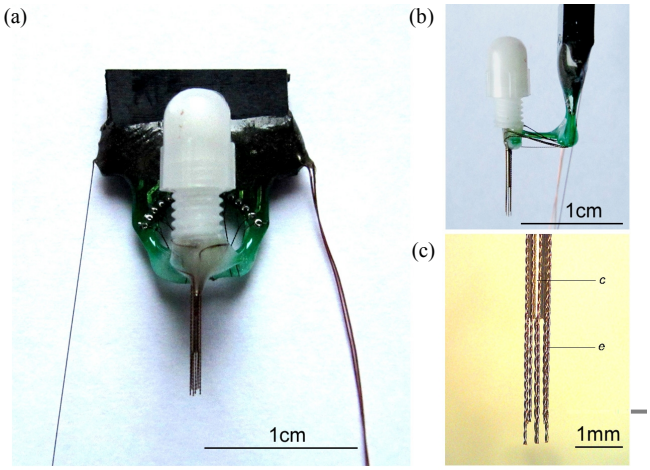

Figure 1. The integrated multi-electrode array coupled with fiberoptic. (a) Frontal view of the array device with cannula cap (instead of optical fiber tail) inserted in the fiber guide cannula. The Omnetics connector was electrically mounted on the PCB skeleton below the connector. The Ref and GND electrodes were arranged at each side of the PCB skeleton. The entire PCB skeleton, including the 16 soldering dots, was coated with insulative glues. (b) Lateral view of the array device. The PCB skeleton formed an L-shaped substrate supporting the guide cannula. (c) Close-up view of the electrode tips. The indicator "c" represents the fiber guide cannula, while "e" indicates the 16 electrodes. It is observed that there exist two categories of electrodes according to the length, and that the electrode tips form Layer 1 and Layer 2, respectively.

B. *Design and Fabrication of the Array Device*

As shown in Figure 1, the integrated device consisted of three components: (1) the framework of the array device for affixing electrodes and optical fiber including the Omnetics connector[11], the fiber guide cannula, and the PCB skeleton as a substrate for the device and conductor for the electrodes; (2) the Nickel-Chromium alloy electrodes with diameter of 35μm and insulative coating; (3) 50/125 (50μm core and 125μm cladding) multimode glass optical fiber tail with FC/PC-typed ceramic plug affixed on its head. The fabrication of the array device started from integrating the PCB skeleton with the Omnetics connector both physically and electrically, followed by bending part of the PCB skeleton to form a L-shaped substrate as shown in Figure 1(b). A fiber guide cannula with entire length of 13.9mm and inner/outer diameter of 300μm/480μm was then clamped and fixed horizontally on the PCB skeleton. In addition, 16 electrodes were prepared that were bundled into 8 electrode pairs for the sake of high tenacity; each electrode pair was cut to a length of ~10cm. Four electrode pairs were arranged cruciformly and sequentially adhered onto the root of the cannula such that each electrode pair clung close and was parallel to the cannula. These first four electrode pairs were cut at the tip with the tips 2.5mm extended the cannula tip, as denoted by "Layer 1". Repeatedly, the other four electrode pairs were adhered onto the root of the cannula with similar arrangement as a counterpart among the space of layer 1. The latter four electrodes were cut and the electrode tips were equally 3.0mm extended the cannula tip and formed "Layer 2". Note that Layer 1 and Layer 2 were parallel with the distance of 0.5mm from each other, where Layer 2 was "deeper" from the cannula tip (see Figure 1c). Besides, two additional electrodes, one for reference (Ref) and another for ground (GND) was connected onto each side of the PCB skeleton respectively. The array device (without the optical fiber) was completed by affixing the fiber cannula guide onto the PCB skeleton, electrically connecting the 16 electrodes and the PCB accordingly, and coating all the soldering dots on the PCB skeleton using insulative glues.

C. *ChR2 Transduction and the Array Device Implantation*

The male SD rats with 180-200g body weight were injected with 1.0 μl AAV2-Syn-ChR2-mcherry virus in dorsolateral periaqueductal gray (dlPAG), which was anterior-posterior (AP) = -7.2mm from bregma and mid-lateral (ML) = -2.0mm from the midline[4]. The surgery of array device implantation was conducted two weeks after the virus injection. The rats were anesthetized, stereotaxically fixed and relocated the PAG area. A round piece of skull of targeted area (diameter = 1.0mm) was carefully removed by means of a craniotomy without damaging the endocranium. For the implantation of the cannula and electrodes, the endocranium was carefully peeled by a needle tip under operating microscope. The array device (without optical fiber) was then stereotaxically implanted through the hole right into the targeted PAG area, with layer 1 recording electrodes located at the central of dlPAG. The Ref electrode was placed between the skull and endocranium, while the GND electrode was bundled sequentially on the cranial nails around. After fastening the array device by filling up the scalp window with dental acrylic, an optical fiber was stereotaxically implanted through the cannula, with the fiber tip 0.5mm above the layer 1 electrode. Rats were allowed to recover for a week before use in the following experiments.

D. *Instrumentation for in vivo Optical Stimulation and Electrical Recording*

The optical path consisted of a 500mW laser, a 3-meter relay optical fiber jumper with 50/125 multimode glass optical fiber. The fiber tail was coupled to the relay fiber jumper at its FC end using a plastic, tube-shaped FC adapter. The laser was triggered by TTL pulses generated by PG4000A digital stimulator (Cygnus Technology Inc.). The laser power at the end of the optical fiber jumper and the laser attenuation of the optical fiber tail were measured by an optical power meter (LTE-1A, Chinese Academy of Sciences, Beijing).

For electrophysiology, the electric signals were recorded and processed by a Plexon Multichannel Acquisition Processor (1-40kHz rate, Plexon Inc., Dallas, TX). Signal preprocessing included calculations on programmable gain and filtering (set at 150–8000Hz band pass) for spikes. Local field potential (LFP) signals were also recorded with band pass filtering at 10-170Hz and digitized at 1kHz sampling rate.

III. RESULTS

A. *Electrical and Optical Characteristics of the Array Device*

To record the extracellular electrophysiological neural activity of the targeted brain area for *in vivo* optogenetics, it is necessary to examine the bandwidth and root-mean-square noise of a single electrode, which in turn are determined by its

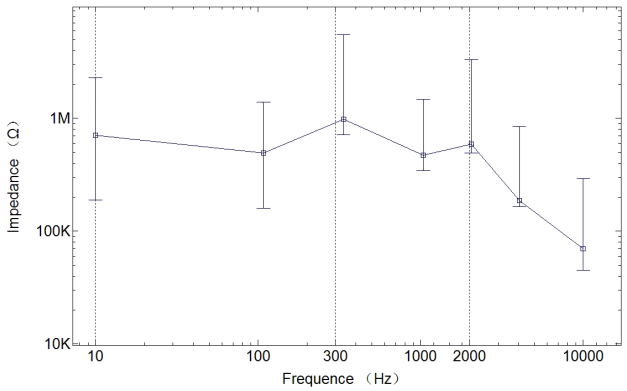

Figure 2. Plot of the average impedance of the 16 electrodes versus frequency. The solid line represents the impedance-frequency polygonal curve, while the straight line segments stand for the error bars of the 16 electrodes.

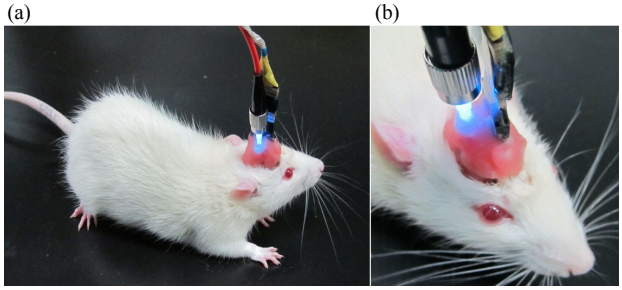

Figure 3. Real picture of the ChR2-transduced rat with the implanted array device during *in vivo* optogenetics. (a) A frontal view of the rat in the experiment of optical stimulation and electrical recording. (b) A close-up view of the rat's head, where both the optical fiber jumper and the Plexon electrical headstage were mechanically mounted on its head, and the implanted array device was coated in dental acrylic, with the Onmetics connector and the FC optical plug outside.

electrical impedance. As shown in Figure 2, the impedance of the electrodes is frequency dependent, varying from 70kΩ to 1MΩ. Especially, for the bands of 300-2kHz and 10-300Hz related to spike and LFP individually, the electrical impedance remains in the range of 400kΩ - 1MΩ, making the multi-electrode array a viable device for both spike and LFP recordings[8].

For neural activity modulation via optogenetics, it is crucial that the light intensity reaches the lower limit for activating the ChR2-transduced neurons, which is $1mW \cdot mm^{-2}$ for blue light as mentioned in other groups' studies[9-10]. Furthermore, the targeted region where ChR2 has been expressed, although depending on the type of viral vector, is typically around $1mm^3$[9]. To ensure the activation of the entire target region, the light intensity with penetration distance z=1mm must reach $1mW \cdot mm^{-2}$. According to the Kubelka-Munk model, we applied Equation (3)-(4) where $S=10.3mm^{-1}$, $n_{tis}=1.36$, $NA_{fib}=0.20$, $r=62.5\mu m$ for 50/125 multimode glass optical fiber. Thus, the light transmission loss at z=1mm was

$$\frac{I(z=1mm)}{I(z=0)} = \frac{0.42^2}{(10.3z+1)(z+0.42)^2}\bigg|_{z=1} = 0.0077 \qquad (5)$$

and the power at the optical fiber tip (P) was

$$P = 1mW \cdot mm^{-2} \times \frac{1}{0.0077} \times \pi r^2 = 1.56mW \qquad (6)$$

The actual light power required for activating the entire ChR2-transduced areas could be derived from Equation (6) by taking into account the light power of the fiber jumper and the laser attenuation at the optical fiber tail. The deduced light power was conformable with the actual power for *in vivo* experiments described below.

B. *Synchronized Optical Modulation and Electrical Recording for in vivo Optogenetics*

In order to test the electrical recording simultaneously with optical stimulation, the ChR2-transduced rats were implanted with the array device. The *in vivo* electrical recording was conducted on free moving rats. After one week recovery from the implantation surgery, the rat was placed into a behavioral rodent resident keeper and connected to the Plexon headstage for electrical recording (see Figure 3). The optical stimulation was triggered and programmed in the form of a train of rectangle pulses with interval of 50ms (20Hz), pulse width of 15ms, and entire duration of 5.0s. The laser power was pre-optimized with each rat to activate freezing or slight flight behavior. The spikes and LFP signals were then recorded with or without laser stimulation, as shown in Figure 4(a)(b). Spike signal was taken into account since the spike firing rate is a critical evaluating indicator for the activation of neurons. The recorded spike activity was shown in Figure 4(c). It was noticed that all the 16 electrodes recorded spikes activity, while 8 out of the 16 electrodes (Ch05, Ch06, Ch07, Ch08, Ch09, Ch10, Ch14, Ch15), with both Layer 1 and Layer 2 involved, recorded significant different spike firing rate during optical stimulation. The spike firing numbers during $[t_0, t_1]$ with no optical stimulus and during $[t_1, t_2]$ with optical stimulus were counted individually for the 16 channels (Fig 4d). Note that for the 8 channels mentioned above, the average spike firing rate during $[t_1, t_2]$ was 9.02/s ("s" for second) whereas the average firing rate during $[t_0, t_1]$ presents was 4.22/s, making it convincing that there exists a significant difference between the spike firing rate data with or without optical stimulation.

In conclusion, we demonstrated here a multi-electrode array device integrated with optical fiber that could be utilized for synchronized electrical recording and optical stimulation of deep brain area on free moving animals. This device is easy to assemble, costless and could be a useful tool for optogenetic studies.

IV. Discussion

In this paper, we developed an integrated device of multi-electrode array coupled with fiberoptic for optical stimulation and electrical recording on free moving animals. We described above the device design and fabrication, the electrical and optical characterization, and *in vivo* optogenetic studies on free moving animals conducted for verification of the array device. The experiments demonstrated the capability

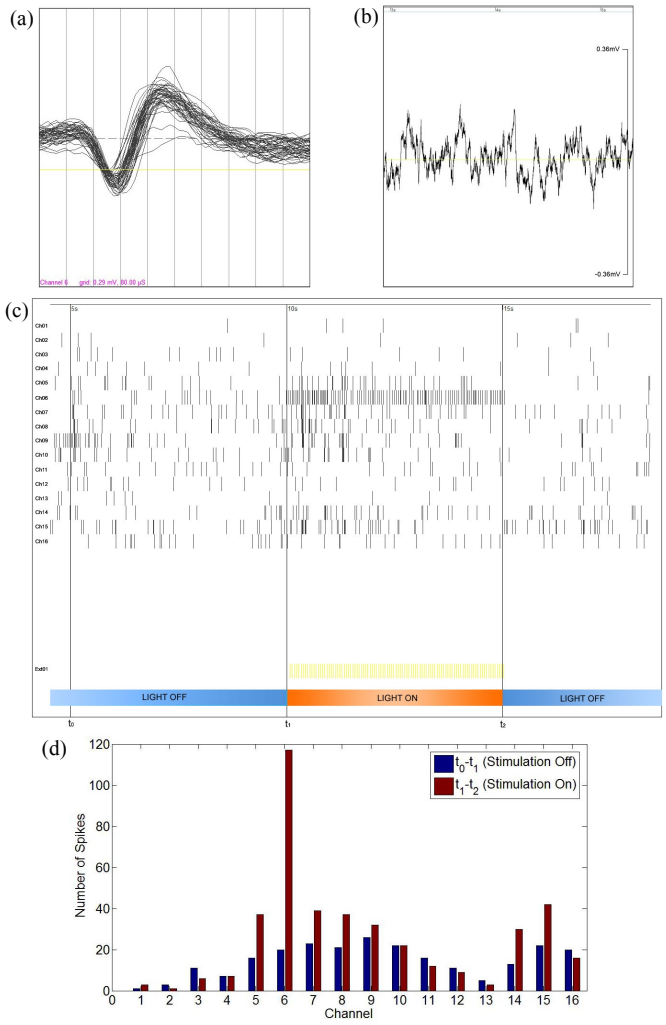

Figure 4. Data on neural signal acquisition and recording for *in vivo* optogenetics. (a)(b) Presentations of spikes and LFPs individually recorded by the array device. (c) The data of spike activity monitored by Plexon software for the 16 electrodes and the triggering signal (Ext01). Time points t_0, t_1, and t_2 were sampled, shown by the three longitudinal straight lines in the figure, and that t_1-t_0=t_2-t_1=5s. During [t_1, t_2] the optical stimulus was triggered on and for other periods shown in the figure the laser was triggered off. (d) Spike numbers for all the 16 channels during [t_0, t_1] (blue bars) and [t_1, t_2] (red bars) that were counted separately.

of the array device upon *in vivo* electrical recording simultaneously with optical stimulation. Unlike the other optical electrode arrays[8-10], our design was able to step further than the surface of brains and was suitable for deep-brain neural modulation and recording simultaneously. Furthermore, the array device was capable of neural signal recording in different depths and horizontal locations, largely owing to the design of two-layer and cruciform-arranged electrodes. With the use of more electrodes, the device can be further improved to have more recording layers. In addition, the cannula designed in the device allowed us either to affix the optical fiber on the device skeleton for chronic study or to probe the optical fiber temporarily for acute recording. Also the cannula can be used for induction of fluidic pharmaceuticals[11], acute implantation of miniature optical microscopes[12], making the array device a available for studies in optogenetic technology, neural engineering, neural pharmacology, and optical neural imaging.

ACKNOWLEDGMENT

The author would like to thank Chaonan Yu for providing technical support on the fabrication of the array device and on part of the surgery for the array device implantation and the *in vivo* experiments.

REFERENCES

[1] Zhang, F., et al., Channelrhodopsin-2 and optical control of excitable cells. Nature Methods, 2006. 3(10): p. 785-792.
[2] Zhang, F., et al., Circuit-breakers: optical technologies for probing neural signals and systems. Nature Reviews, 2007. 8: p. 577-581.
[3] Kravitz, A.V. and A.C. Kreitzer, Optogenetics manipulation of neural circuitry *in vivo*. Current Opinion in Neurobiology, 2011. 2011(21): p. 433-439.
[4] Cardin, J.A., et al., Targeted optogenetic stimulation and recording of neurons *in vivo* using cell-type-specific expression of Channelrhodopsin-2. Nature Protocol, 2010. 5(2): p. 247-254.
[5] Aghagolzadeh, M., F. Zhang, and K. Oweiss, An implantable VLSI architecture for real time spike sorting in cortically controlled brain machine interfaces, in 32nd Annual International Conference of the IEEE EMBS. 2010: Buenos Aires, Argentina. p. 1569-1572.
[6] Nordhausen, C.T., E.M. Maynard, and R.A. Normann, Single unit recording capabilities of a 100 microelectrode array. Brain Research, 1996. 726(1996): p. 129-140.
[7] Stieglitz, T. and M. Gross, Flexible BIOMEMS with electrode arrangements on front and back side as key component in neural prosthesis and biohybrid systems. Sensors and Actuators B, 2002. 83(2002): p. 8-14.
[8] Zhang, J., et al., A microelectrode array incorporating an optical waveguide device for stimulation and spatiotemporal electrical recording of neural activity, in 31st Annual International Conference of the IEEE EMBS. 2009: Minneapolis, Minnesota, USA. p. 2046-2049.
[9] Aravanis, A.M., et al., An optical neural interface: *in vivo* control of rodent motor cortex with integrated fiberoptic and optogenetic technology. Journal of Neural Engineering, 2007. 4(2007): p. 143-156.
[10] Wang, J., et al., Integrated device for combined optical neuromodulation and electrical recording for chronic *in vivo* applications. Journal of Neural Engineering, 2012. 9(2012): p. 1-14.
[11] Rubehn, B., et al., Polymer-based shaft microelectrodes with optical and fluidic capabilities as a tool for optogenetics, in 33rd Annual International Conference of the IEEE EMBS. 2011: Boston, Massachusetts, USA. p. 2969-2972.
[12] Davis, M.D. and J.J. Schmidt, *In vivo* spectrometric calcium flux recordings of intrinsic caudate-putamen cells and transplanted IMR-32 neuroblastoma cells using miniature fiber optrodes in anesthetized and awake rats and monkeys. Journal of Neuroscience Methods, 2000. 99(2000): p. 9-23.